Available online at www.sciencedirect.com
SCIENCE DIRECT
C. R. Mecanique 333 (2005) 804–809
COMPTES RENDUS MECANIQUE
http://france.elsevier.com/direct/CRAS2B/

On mode localisation in tensile plate buckling

Nicolas Jacques *, Michel Potier-Ferry

Laboratoire de Physique et Mécanique des Matériaux (LPMM), UMR CNRS 7554, Université Paul-Verlaine, île du Saulcy, 57045 Metz cedex 01, France

Received 19 July 2005; accepted 11 October 2005

Presented by Huy Duong Bui

Abstract

In some cases, a tensile load may induce small compressive stresses and buckling phenomenon. In this Note, we present an analytical study of the buckling of long stretched plates. From this analytical model, one explains the wavelength selection and establishes that the in-plane stress localisation induces the mode localisation. Comparison with numerical results shows a good agreement. ***To cite this article: N. Jacques, M. Potier-Ferry, C. R. Mecanique 333 (2005).***
© 2005 Académie des sciences. Published by Elsevier SAS. All rights reserved.

Résumé

Flambement localisé de bandes sous traction. Cet article porte sur le flambement de bandes longues induit par des contraintes compressives secondaires apparaissant lors de l'application d'un chargement de traction. Un modèle analytique a été mis au point. Il permet d'expliquer la forme caractéristique des modes lors de ce type de flambement. Elle est principalement due à la localisation des contraintes compressives et à l'existence d'un mécanisme de sélection des longueurs d'onde. Ces résultats sont validés par des calculs par éléments finis. ***Pour citer cet article : N. Jacques, M. Potier-Ferry, C. R. Mecanique 333 (2005).***
© 2005 Académie des sciences. Published by Elsevier SAS. All rights reserved.

Keywords: Solids and structures; Buckling; Thin plates; Wavelength selection; Mode localisation

Mots-clés : Solides et structures ; Flambement localisé ; Plaques minces ; Sélection des longueurs d'ondes

1. Introduction

The buckling of structures due to compressive loads is a well-known problem. A tensile loading can also induce buckling. Indeed, for some structures, application of a tensile load leads to the occurrence of compressive stresses generally perpendicular to the main loading direction. The most famous example is the Yoshida buckling test [1], where a square plate is subjected to a diagonal tension inducing an inhomogeneous stress field. Another example is proposed by Timoshenko and Goodier [2], who study a rectangular plate subjected to a parabolic traction on two opposite sides. They observe the occurrence of transverse compressive stresses. Friedl et al. [3] consider the buckling of stretched strips with special boundary conditions that constrain the lateral displacements on the loaded edges and

* Corresponding author.
E-mail address: jacqueni@lpmm.univ-metz.fr (N. Jacques).

1631-0721/$ – see front matter © 2005 Académie des sciences. Published by Elsevier SAS. All rights reserved.
doi:10.1016/j.crme.2005.10.013

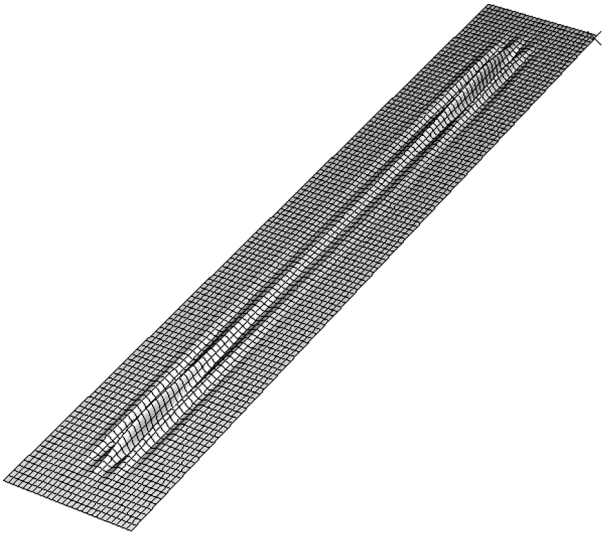

Fig. 1. Buckling of a stretched strip, from [3]. The load is applied in the longitudinal direction, the lateral displacements are prevented on the short edges and the long edges are free. The aspect ratio is seven.

Fig. 1. Flambage d'une plaque sous traction, d'après [3]. Le chargement est appliqué selon la longueur, les conditions aux limites empêchent tout déplacement latéral au niveau des cotés les plus courts, les autres bords sont libres. La longueur de la plaque est égale à sept fois sa largeur.

lead to transverse compressive stresses near these edges. Fig. 1 shows a buckling mode obtained by Friedl et al. [3] with use of a finite element analysis. Long waves are present near the centreline and the displacement is larger in the area where compressive stresses reach their maximum value. Far from the loaded edges, where the transverse stresses are vanished, buckles decay.

In this paper, we propose an analytical study of the buckling of long plates under global tension. We point out that the buckling mode localisation is induced by the localisation of the in-plane compressive stresses.

2. Governing equations

We considerer a rectangular plate of thickness t, width B and length L, with $t \ll B < L$. x and y denote the in-plane coordinates, x in the longitudinal direction, y in the transverse direction such that the domain is $0 \leqslant x \leqslant L$, $-B/2 \leqslant y \leqslant B/2$. We assume an elastic isotropic behaviour with E the Young's modulus and ν the Poisson's ratio. A tensile load is applied on the short lateral edges. Since inhomogeneous loading or special boundary conditions are considered, a complex membrane force field (1) appears. In the framework of a linear buckling analysis, this pre-buckling stress field (1) is assumed to be proportional to the applied traction.

$$\big[N(x,y)\big] = \begin{bmatrix} N_x(x,y) & N_{xy}(x,y) \\ N_{xy}(x,y) & N_y(x,y) \end{bmatrix} \tag{1}$$

If the length L is sufficiently large, the Saint-Venant's principle implies that, far from the loaded edges, the traction becomes uniform, i.e. only the longitudinal membrane forces N_x are non-zero and are constant through the width. So, transverse forces are located near the short edges.

It is well known that bifurcation occurs when the quadratic part of the potential energy P_2 changes sign, i.e. $P_2 = 0$ and $\delta P_2 = 0$. In the context of a thin plate model, the quadratic part of the potential energy reduces to:

$$2P_2 = \int_S \left(D(\Delta w)^2 + N_x \left(\frac{\partial w}{\partial x}\right)^2 + N_y \left(\frac{\partial w}{\partial y}\right)^2 + 2N_{xy} \frac{\partial w}{\partial x} \frac{\partial w}{\partial y} \right) \mathrm{d}x\, \mathrm{d}y \tag{2}$$

where $w(x,y)$ is the out-of-plane displacement. D is the bending stiffness modulus (3).

$$D = \frac{Et^3}{12(1-\nu^2)} \tag{3}$$

The first term of the right-hand side of Eq. (2) corresponds to the elastic bending stiffness, the three other terms to the stress stiffness.

Owing to the characteristics of the considered buckling problems, we propose some approximations:

- The dominant term in the elastic energy is due to the shell curvature in the transverse direction. Indeed, Fig. 1 shows that the wavelength in the y-direction is very much shorter than in the x-direction. The term $D(\Delta w)^2$ in Eq. (2) is replaced by $D(\partial^2 w/\partial y^2)^2$.
- For the same reason, the mode shape implies that $(\partial w/\partial x) \ll (\partial w/\partial y)$. Since the shear and lateral stresses are of the same order of magnitude, then the contribution of the shear stresses to the quadratic part of the potential energy (2) is negligible compared to the lateral stresses contribution.
- The variation of the longitudinal tensile stresses is small compared to their mean value, so that: $N_x(x, y) = N_x$.
- We assume cellular buckling $w(x, y) = \cos(ky)F(x)$. $F(x)$ represents the buckling mode in the longitudinal direction. With this approximation, the decay of the buckling patterns in the y-direction is disregarded. So, the decrease of the lateral stresses should also not be taken into account. For this reason, we assume $N_y(x, y) = -\lambda \Sigma_y(x)$. λ denotes the magnitude of the transverse compressive forces, $\Sigma_y(x)$ is a normalized function representing the variation of this component in the x-direction along the centreline, $\max(\Sigma_y) = 1$. Hence, the proposed analytical approach is representative of the buckling patterns located near the longitudinal plate centreline, i.e. where the compressive stresses and the buckles amplitude are maximum. This hypothesis is valid if the transverse wavelength is small compared to the strip width.

With these hypotheses, Eq. (2) can be rewritten as ($m = L/2$):

$$\frac{2P_2}{B} = Dk^4 I_1 + N_x I_3 - \lambda k^2 I_2 \tag{4}$$

with $I_1 = \int_0^m F^2 \,\mathrm{d}x$, $I_2 = \int_0^m \Sigma_y F^2 \,\mathrm{d}x$ and $I_3 = \int_0^m (\partial F/\partial x)^2 \,\mathrm{d}x$.

Stationarity of the potential energy (4) ($\delta P_2 = 0$) leads to the following differential equation:

$$-N_x\left(\frac{\partial^2 F}{\partial x^2}\right) + \left(Dk^4 - \lambda k^2 \Sigma_y(x)\right)F = 0 \tag{5}$$

In general, Eq. (5) has no analytical solution. Nevertheless, if the transverse compressive stresses are zero, $\Sigma_y(x) = 0$, Eq. (5) has the following symmetric solution:

$$F(x) = \mathrm{e}^{-c(x-m)} + \mathrm{e}^{c(x-m)} \quad \text{with } c = \sqrt{\frac{D}{Nx}}k^2 \tag{6}$$

The solution (6) describes the decrease of the buckles amplitude far from the loaded edges where the lateral stresses are vanished.

3. Mode localisation

The considered problem has no analytical solution. Here, the critical tensile load and the mode shape are determined with use of a Ritz method (see, e.g. [4]). A trial function $F(x)$ depending of several parameters c_i is used as an approximation for the buckling mode in the x-direction. An example of such trial function is presented at the end of this section. From the buckling condition, $P_2 = 0$, an expression of the critical compressive membrane force is obtained for a given mode shape:

$$\lambda = \frac{1}{I_2}\left(k^2 D I_1 + \frac{N_x I_3}{k^2}\right) \tag{7}$$

By minimizing λ with respect to k ($\partial\lambda/\partial k = 0$), we obtain the expression of the transverse wavenumber and of the corresponding critical membrane force:

$$k^4 = \frac{N_x I_3}{D I_1} \tag{8}$$

$$\lambda = Tg\sqrt{DN_x} \quad \text{with } Tg = 2\frac{\sqrt{I_1 I_3}}{I_2} \tag{9}$$

The transverse buckling wavenumber k results from two stabilizing mechanisms: on the one hand, the wavelength increases with the bending stiffness modulus. On the other hand, a higher value of the longitudinal transverse stress leads to a shorter wavelength [5]. A similar wavelength selection mechanism occurs in the buckling of a compressed beam on an elastic foundation. Moreover, note that the ratio $\sqrt{I_1/I_3}$ depends only on the function $F(x)$. It corresponds to the characteristic length of the buckling mode in the longitudinal direction. We adopt the notations $k_x = \pi/l_x = \sqrt{I_3/I_1}$ and $\sigma_x = N_x/t$. With use of Eq. (3), Eq. (8) can be rewritten as

$$k^4 = 12(1-\nu^2)\frac{\sigma_x}{E}\left(\frac{k_x}{t}\right)^2 \tag{10}$$

This expression shows that the mode localisation in the transverse direction, characterized by the wave number k, increases for higher values of the tensile stress, lower values of the sheet thickness, and higher values of k_x, which characterizes the mode localisation in the x-direction.

The mode shape in x-direction is determined by minimizing λ with respect to the parameters c_i of the trial function $F(x)$.

$$\lambda^{\text{crit}} = Tg^{\min}\sqrt{DNx} \quad \text{with } Tg^{\min} = \min_{F(x)}(Tg) \tag{11}$$

Tg depends only on the functions $\Sigma_y(x)$ and $F(x)$. This provides an important result: the mode shape in the longitudinal direction depends only on the distribution of the compressive stresses in this direction. In other words, the localisation of the transverse compressive stresses induces the mode localisation. The quantity $2\pi/Tg^{\min}$ is dimensionally similar to a length and defines the characteristic length l_c of the compressed area.

$$l_c = \frac{2\pi}{Tg^{\min}} = \pi\frac{I_2}{\sqrt{I_1 I_3}} \tag{12}$$

For example, with a uniform compressive membrane force, $\Sigma_y(x) = 1$, the problem has an exact solution: $F(x) = \cos(\pi x/L)$. In this case, we find $l_c = L$ and $l_x = L$. With the notation (12) and Eqs. (3), (11), we deduce the critical transverse stress as a function of the ratio t/l_c:

$$\left|\sigma_y^{\text{crit}}\right| = \frac{\lambda^{\text{crit}}}{t} = \pi\sqrt{\frac{E\sigma_x}{3(1-\nu^2)}}\frac{t}{lc} \tag{13}$$

If the compressive stresses are due to the tensile load, assuming a linear behaviour of the structure in the pre-buckling stage, longitudinal and transverse stresses are proportional, thus:

$$\frac{|\sigma_y|}{\sigma_x} = C \tag{14}$$

Therefore, the expression for the critical tensile stress and the associated transverse wavelength are obtained:

$$\sigma_x^{\text{crit}} = \frac{N_x^{\text{crit}}}{t} = \frac{E\pi^2}{3(1-\nu^2)C^2}\left(\frac{t}{lc}\right)^2 \quad \text{and} \quad l = \frac{2\pi}{k} = \sqrt{2Cl_x l_c} \tag{15}$$

Buckling of plates involves generally a slenderness ratio of the structure. In this case, this is the ratio between the thickness t and the characteristic length l_c of the compressed area. If the plate is long enough, the compressive stresses localisation implies that the critical tensile stress is independent of the plate length, see also [3]. In addition, the pre-buckling problem is two-dimensional, so the coefficient C and the shape of the compressed area are independent of the shell thickness. As mentioned above, the mode shape in the x-direction depends only on the shape of the transverse stress field in this direction. So, the expression of the transverse wavelength (15) shows that the mode shape is independent of the shell thickness. Moreover, the important difference between the transverse wavelength l and the longitudinal buckling length l_x is mainly due to the small values of C, see the next section.

In order to apply the proposed analytical approach, we adopt the following expression for the trial function $F(x)$ to describe the evolution of the buckles amplitude in the x-direction:

$$\begin{cases} F(x) = 0 & \text{for } x \leqslant b \\ F(x) = \left(1 - \mathrm{e}^{-(a(x-b))^2}\right)\left(\mathrm{e}^{-c(x-m)} + \mathrm{e}^{c(x-m)}\right) & \text{for } x > b \end{cases} \tag{16}$$

This function depends on three parameters: a, b and c. The integrals I_1, I_2 and I_3 have no analytical expressions and are evaluated numerically. The values of the parameters a, c and b which minimize Tg (9) are determined with use of optimisation techniques (Newton's algorithm).

4. Comparison with finite element solutions

Results derived from the analytical approach are compared with results of numerical buckling analyses. Computations are performed with the software ABAQUS. The plate is meshed with S8R5 shell elements. They are quadratic elements with reduced integration, dedicated to thin shell problems. So, the transverse shear flexibility is neglected. To apply the analytical approach, we need to the shape of the transverse stresses, $\Sigma_y(x)$, and C, the ratio between the lateral compressive stresses and the global tension. There are provided by a linear static finite element calculation. Three configurations have been studied:

(a) The first configuration corresponds to an example proposed by Friedl et al. [3]. It is a rectangular plate subject to a longitudinal tension. The long edges are free. On the short edges, the lateral displacement is prevented and the longitudinal displacement is uniform. The following geometry is considered: $L = 1400$ mm, $B = 200$ mm and $t = 0.05$ mm. The material behaviour is linear isotropic elastic with $E = 70\,000$ MPa and $\nu = 0.3$. In this case, the ratio C is about 5.7×10^{-3}. The mode shape is plotted in Fig. 1.

(b) The second configuration has the same geometry with a transversely isotropic elastic behaviour: $E_x = 50\,000$ MPa, $E_y = 18\,182$ MPa, $\nu_{xy} = 0.3$, $\nu_{yx} = 0.099$ and $G_{xy} = 6993$ MPa. The transverse bending stiffness has the following expression:

$$D = \frac{E_y t^3}{12(1 - \nu_{xy}\nu_{yx})} \tag{17}$$

For this configuration, the ratio C is about 8.4×10^{-4}.

(c) For the third example, another transversely isotropic elastic behaviour is considered: $E_x = 18\,182$ MPa, $E_y = 50\,000$ MPa, $\nu_{xy} = 0.099$, $\nu_{yx} = 0.3$ and $G_{xy} = 6993$ MPa. C is about 2.5×10^{-3}.

Analytical and numerical results for the critical membrane force and the mode shape are presented in Table 1. The evolution of the buckling modes derived from the two methods and the compressive stress field are plotted in Fig. 2. A good agreement between analytical and numerical results is found. For the critical load, the difference is less than 10%. Fig. 2 shows the influence of the localisation of the compressive stresses on the mode shape. The out-of-plane displacement is maximum where these stresses have a significant value. The buckling affects an area that is about twice larger than the compressed area. Note that the mode localisation is well predicted by the analytical approach.

Table 1
Comparison between results of the proposed analytical approach (Ana.) and the finite element method (FE)

Tableau 1
Comparaison entre résultats analytiques (Ana.) et numériques (FE)

Configuration (a)							
	N_x^{crit} (N/mm)	l (mm)	a (mm^{-1})	c (mm^{-1})	b (mm)	l_c (mm)	l_x (mm)
Ana.	31.7	26.5	0.00728	0.0089	69	175	351
FE	34.95	≈26					
Configuration (b)							
	N_x^{crit} (N/mm)	l (mm)	a (mm^{-1})	c (mm^{-1})	b (mm)	l_c (mm)	l_x (mm)
Ana.	184.5	15.1	0.0054	0.0054	79	242	558
FE	189.6	≈14.8					
Configuration (c)							
	N_x^{crit} (N/mm)	l (mm)	a (mm^{-1})	c (mm^{-1})	b (mm)	l_c (mm)	l_x (mm)
Ana.	187.1	14.2	0.00944	0.0104	48	138	285
FE	194.2	≈16					

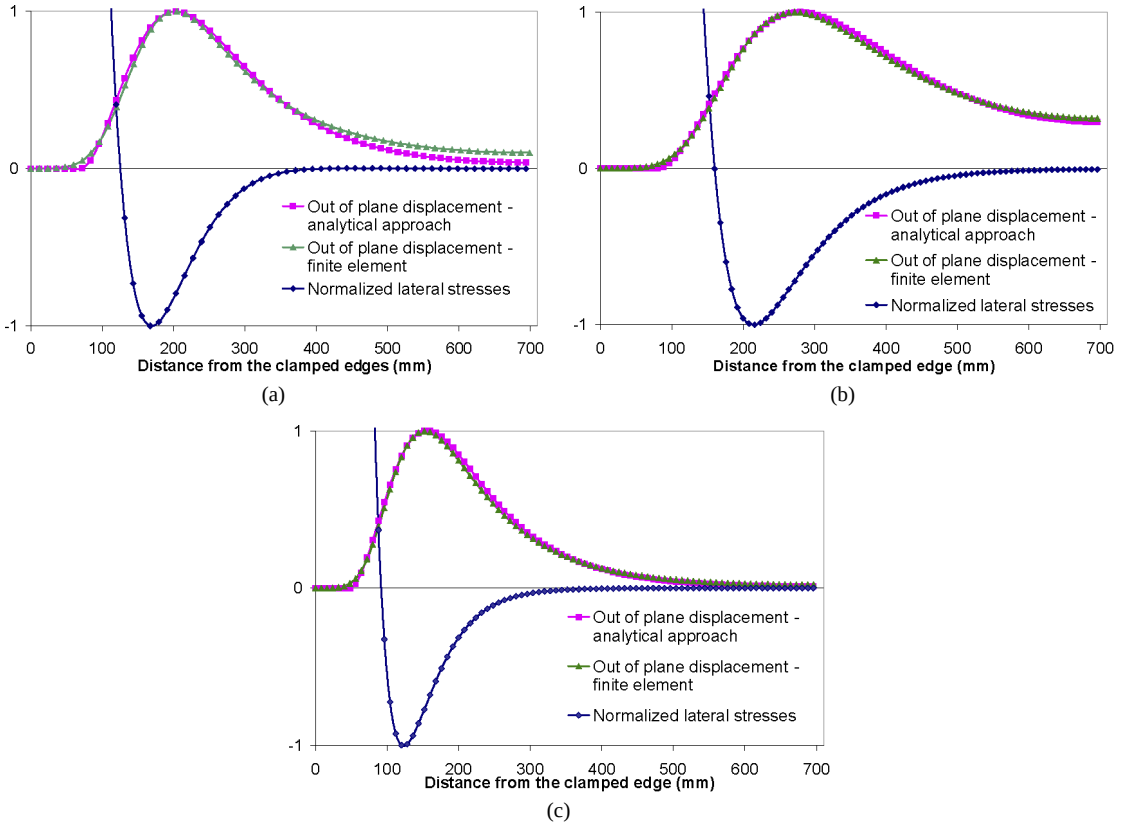

Fig. 2. Evolution of the lateral compressive stresses and the buckling mode in the longitudinal direction. Mode shape predictions based on the analytical approach are compared with finite element simulations. For the finite element solutions, curves correspond to stresses and displacements along the centreline. Data for the three configurations (a), (b) and (c) are presented in the third paragraph.

Fig. 2. Répartition des contraintes compressives et forme du mode de flambage dans le sens long. La forme du mode est déterminée à la fois par l'approche analytique et par des calculs par éléments finis. Les résultats numériques correspondent aux contraintes et déplacements le long de la ligne médiane de la plaque. Données des configurations (a), (b) et (c) : cf. paragraphe 3.

5. Conclusions

This paper deals with tensile plate buckling. This phenomenon occurs when a tensile load causes small lateral compressive stresses. An analytical procedure is proposed to compute the critical magnitude of a given stress field. The results are in good agreement with numerical solutions. This study highlights the main features of this kind of buckling. The important difference between the characteristic buckling lengths in transverse and longitudinal directions is due to the small level of the compressive stresses compared to the global tension. We observe that the localisation of the compressive stresses induces the mode localisation.

References

[1] K. Yoshida, J. Hayashi, M. Hirata, Yoshida buckling test, IDDRG, Kyoto, Japan, 1981.
[2] S.P. Timoshenko, J.N. Goodier, Theory of Elasticity, McGraw-Hill, 1982.
[3] N. Friedl, F.G. Rammerstorfer, F.D. Fisher, Buckling of stretched strips, Comput. Struct. 78 (2000) 185–190.
[4] F.D. Fisher, F.G. Rammerstorfer, N. Friedl, W. Wieser, Buckling phenomena related to rolling and levelling of sheet metal, Int. J. Mech. Sci. 42 (2000) 1887–1910.
[5] E. Cerda, L. Mahadevan, Geometry and physics of wrinkling, Phys. Rev. Lett. 90 (2003) 074302.